

2-D Islanding of Dodecane on an Au(111) Surface: An Investigation Using He Beam Reflectivity and Monte Carlo Modeling[†]

Timothy C. Arlen,[‡] Craig J. D. Webster,[§] and Peter V. Schwartz^{*,‡}

Physics Department, California Polytechnic State University, San Luis Obispo, California 93401, and Physics Department, Princeton University, Princeton, New Jersey 08544

Received: August 1, 2007; In Final Form: October 14, 2007

Dodecane is deposited at submonolayer coverages onto an Au(111) surface forming two-dimensional (2-D) islands. The islands sublime to a 2-D gas at higher substrate temperatures. We observe island formation and subsequent 2-D sublimation between substrate temperatures of 40 and 350 K, using low-energy helium reflectivity. A computer model of the submonolayer islanding process using Monte Carlo simulations shows significant agreement with experimental data and yields an intermolecular potential of 0.10 ± 0.03 eV (about half that of the bulk substance) and a significantly higher corrugation potential of 0.3 ± 0.1 eV.

Introduction

Just as the process of sublimation in three dimensions is of interest from the perspective of intermolecular attraction and entropy, the two-dimensional (2-D) analogue is intriguing with the added consideration of molecular interaction with the substrate. Over the past few decades, there has been an increasing amount of interest in molecular ordering processes on surfaces.^{1–3} Furthermore, this interplay between van der Waals forces and entropy due to thermal energy dominates considerations of molecular biology and self-assembly.^{4,5} Besides being of interest from a basic science standpoint, this phenomenon of surface ordering has shown technological promise as well, playing a significant role in the fields of nanotechnology and rheology.^{6–9}

In a recent AFM study,¹⁰ it was shown that lateral force microscopy can directly visualize a gas phase of adsorbed long-chain alcohols and fatty acids. The 2-D gas originated from the edge evaporation of dense solid phase island domains deposited on a mica surface via microcontact printing. We extend this research by observing a 2-D sublimation process in real time as a function of substrate temperature using helium atom reflectivity, which is perfectly surface sensitive and non-perturbative. A simple Monte Carlo model allows the quantitative determination of two energies: the intermolecular potential between two dodecane molecules on the Au(111) surface and the corrugation energy of dodecane on the Au(111) surface.

Our observational technique exploits the non-reflectivity of organic molecules. The reflectivity of the gold surface is reduced by more than 3 orders of magnitude when covered with an organic monolayer. Additionally, long-range forces cause a single molecule on the surface to reduce reflectivity by significantly more than just the molecular footprint. A single molecule of radius r and area πr^2 would impede the reflectivity of the substrate over its scattering cross-sectional area, $\Sigma = \pi(r + \phi)^2$, where ϕ is the width of the molecular shadow surrounding the particle. We have measured this enhanced scattering cross-section of dodecane to be approximately 9 times

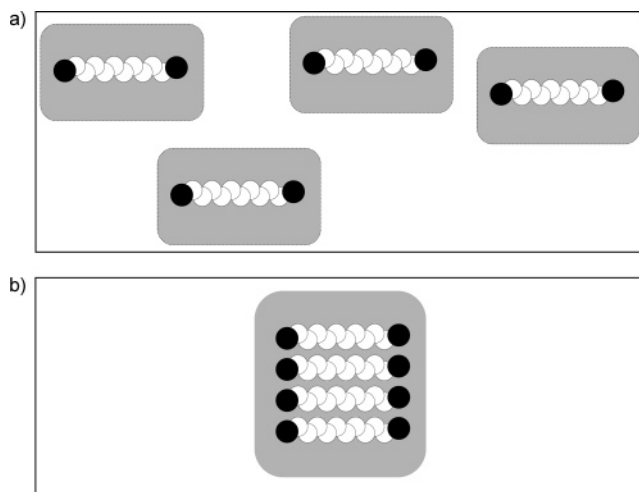


Figure 1. (a) Molecule's shadow or footprint is about 9 times the molecular area, resulting in a reflectivity of about 50% for this surface. (b) When the molecules are ordered, the overlap of the shadow region results in a reflectivity increase to about 75%.

the actual molecular footprint, consistent with previous studies.¹¹ However, when the molecules are closely packed in well-ordered islands, the molecular shadows overlap and the scattering cross-section is not much larger than the footprint of the island as a whole. Therefore, the reflectivity of a gold surface with submonolayer coverage increases as the molecules order (Figure 1).

This technique can be used to convey information about the degree of 2-D islanding on the surface. Two sets of specular data are obtained: (1) heating/cooling curves record the near equilibrium specular intensity as the temperature of the crystal surface is slowly heated or cooled and (2) specular recovery curves measure the specular intensity versus time immediately after dodecane is applied to a bare gold surface, providing real time ordering information for different substrate temperatures.

Experimental Procedures

The general layout of the helium beam surface diffraction apparatus has been previously described in several publications.¹² Briefly, the scattering apparatus consists of two differ-

[†] Part of the "Giacinto Scoles Festschrift".

[‡] California Polytechnic State University.

[§] Princeton University.

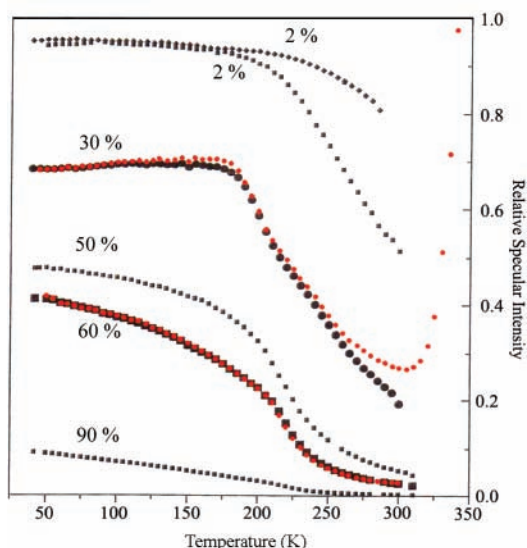


Figure 2. Reflectivity vs temperature curves for six different coverages. Black dots indicate decreasing temperature. In two instances, the temperature was increased again (red dots).

entially pumped vacuum chambers. In the first, a helium beam is produced by supersonic expansion from a cold source into a background pressure of approximately 10^{-4} Torr. The source temperature is usually maintained at 70 K, corresponding to a wave vector of 53 nm^{-1} . The beam then passes through the skimmer into the second chamber with a base pressure of 10^{-7} Torr, where it strikes a crystal mounted on a manipulator. A rotating bolometer, in thermal contact with a 1.6 K pumped helium cryostat, detects the beam signal. The detector/crystal assembly is located inside two concentric radiation shields cooled with liquid nitrogen, which keep thermal radiation from warming the bolometer (and its cryostat) and define an inner space that is very effectively cryopumped, keeping estimated pressures of impurities as low as 10^{-12} Torr near the crystal when the cryostat is at 1.6 K.

We obtained a clean gold surface via argon sputtering and annealing as described elsewhere¹² and confirmed surface cleanliness by observation of gold reconstruction.¹³ Dodecane flux to the surface was calculated using the vapor pressure of the decanethiol (kept at a constant temperature in a reservoir) and the geometry of the dosing mechanism. The flux was also measured by observation of specular attenuation after dosing to a cold gold surface. The interior of the scattering chamber was kept at 77 K so each dose ended immediately after the shutter closed.

Data were collected in two ways: (1) specularly was recorded as a function of temperature immediately after molecular deposition at 300 K for doses of a wide range of coverages (Figure 2). The substrate was immediately cooled at a rate of $\sim 0.2 \text{ K/s}$ (black dots in Figure 2). In two instances, the sample was subsequently heated again to room temperature at a rate of 1 K/s (red dots in Figure 2) and (2) specularity was recorded as a function of time for different substrate temperatures immediately after a molecular deposition of $\sim 5\%$ coverage (Figure 3)

Results and Discussion

Near equilibrium reflectivity curves were recorded for six different molecular coverages (Figure 2). Higher coverages reveal less bare gold and thus have a lower reflectivity. Additionally, as the surface temperature decreases (black dots

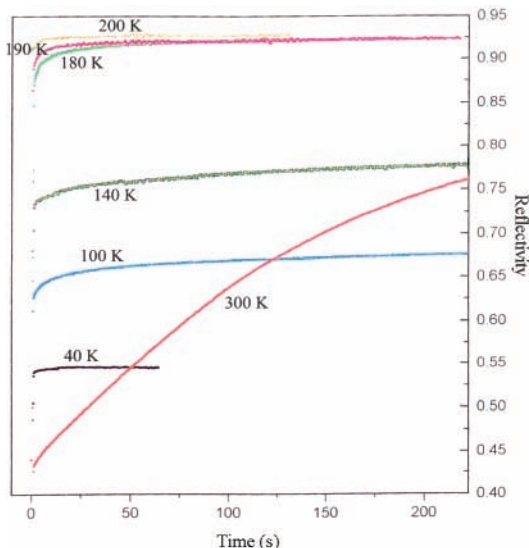


Figure 3. Reflectivity vs Time curves immediately after a molecular dose of about 5% coverage onto a clean Au(111) surface. Crystal temperature is indicated by each curve.

in Figure 2), there is a transition to higher specularity as the 2-D gas of the surface molecules orders into large islands, allowing the shadow regions of each molecule to overlap (see Figure 1). The specularity is essentially proportional to the surface area of clean, bare gold. Thus, at 40 K conditions (large, ordered molecular islands), the coverage can be best estimated as

$$\Theta \approx 1 - S_{\text{Au}}$$

where S_{Au} is the specularity (at 40 K) relative to the bare gold surface (y-axis, Figure 2). For the two coverages, the sample temperature was increased back to room temperature at a rate of about 1 K/s . The close agreement between heating and cooling during the transition phase implies near equilibration in this regime. The increase in specularity of the 30% coverage trace at higher temperatures is due to a loss of molecules as the dodecane molecules desorbed from the gold surface.

The reflectivity versus time curves (Figure 3) show an increase in specularity over time as the molecules order into islands of various sizes on the gold surface. The 300 K trace is an exception: the specularity increases with the loss of molecules from the gold surface due to dodecane desorption. Figure 2 indicates that the ultimate (equilibrium) reflectivity should be near maximum for crystal temperatures less than 180 K. However, we are never able to see these higher reflectivities for lower temperature depositions because the transition to order is prohibitively slow. A study by Stranick et. al¹⁴ indicates that molecules deposited onto a 4 K surface are able to migrate a maximum of four lattice spaces before thermalizing and remaining trapped in the corrugation potential. Thus, the marginal increase in reflectivity for lower temperature depositions may be due to some molecules hopping to a nearly terrace step edge, pairing with another molecule or grouping into small islands before becoming kinetically trapped in an unequilibrium state. Only for the 180, 190, and 200 K traces is transition to equilibrium observed. Additionally, the transition takes place slightly slower for the 180 K trace as one would expect.

Computer Model

To interpret the data and extract quantitative information, a Monte Carlo model was developed to provide simulated specular recovery curves and specularity versus temperature curves.

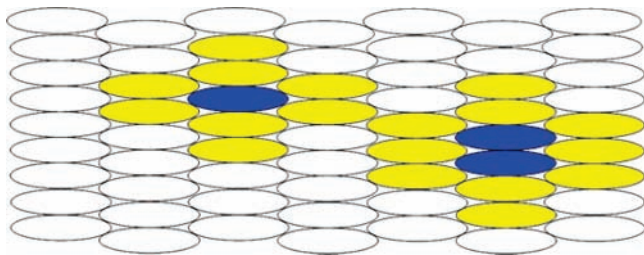


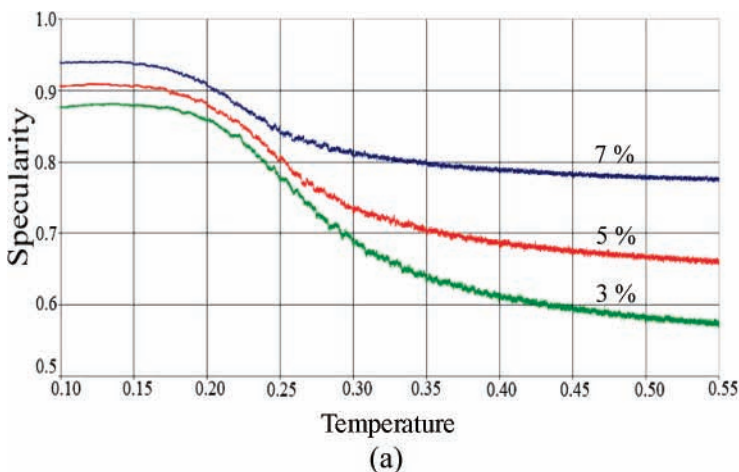
Figure 4. Dodecane molecules (blue) in a hexagonal array of possible locations. Yellow sites represent sites that are shadowed (rendered unreflective) due to the long-range molecular attraction between the dodecane molecule and the incident helium atoms.

The molecules are modeled as point particles on a hexagonal lattice with periodic boundary conditions. Each molecule on the (500×500) lattice is allowed to interact with its six nearest neighboring sites, consistent with hexagonal mesh of the dodecane monolayer¹⁵ (Figure 4). The six nearest neighbors are the four termina neighbors (having contact only via the terminal methyl groups) and the two lateral neighbors (contacting via the long side of the molecule). The shadowing effect is accounted for in the following way: the ratio of the scattering cross-section (Σ) to the molecular footprint (A) is $\Sigma/A = 9$, consistent with our experimental measurements and previous studies.¹¹ The entire area that is rendered unreflective is the molecule itself, all four termina neighbors, the two lateral neighbors, and the two next nearest lateral neighbors.

A lateral neighbor attraction (corresponding to two molecules lying next to each other, sharing their long side) has a strength of ϵ , which is 6 times that of a termina neighbor (corresponding to attraction between terminal methyl groups). This 1:6 ratio was derived from desorption energies dependent on chain length.¹⁶ A molecule and (vacant) neighboring site were chosen at random. The molecule moves to the adjacent site if the move represents a lower energy or equal energy state. If the move represents an increase in energy, the molecule is allowed to move with a probability given by the Boltzmann factor

$$P(E) = e^{-E/k_B T} \quad (1)$$

where E is the increase in energy required for the move. Using the computer model, specularity versus time and specularity versus temperature curves were generated (see Figure 5) and can be compared to the experimental data. These comparisons allow us to calculate values of the intermolecular potential and corrugation energy of dodecane on the Au(111) surface.



In Figure 5a, the model was cooled at a rate of 1 million iterations per ϵ/k_B (our model temperature unit, see following discussion). The trends in Figure 5a are reasonably consistent with the data in Figure 2. By locating the knee of the simulated cooling curve and comparing it to the knee of the experimental cooling curve, we were able to estimate the interaction energy of a lateral bond between two molecules using the model

$$T_{\text{knee}} = 0.18 \epsilon/k_B \quad (2)$$

where ϵ is the interaction energy of a lateral bond and $\epsilon/6$ is the energy associated with a termina bond. Thus, by locating the experimental temperature at the knee and comparing it to the model's temperature at the knee, we can calculate ϵ in the following way:

$$0.18 \frac{\epsilon}{k_B} = 200 \text{ K} \Rightarrow \epsilon = \frac{200 \text{ K}(k_B)}{0.18} \approx 0.10 \text{ eV} \quad (3)$$

Thus, we estimate that the lateral interaction energy is 0.10 ± 0.03 eV. The uncertainty is primarily due to uncertainties in the exact location of the knee.

By using the enthalpy of desorption of bulk dodecane of 1.0 eV,¹⁶ the intermolecular potential of the lateral bond in bulk can be estimated to be 0.21 eV or about twice what we calculated. This discrepancy may be explained by the difference in lateral spacing on a corrugated gold surface versus molecules in bulk dodecane. The intermolecular spacing in bulk (d_b) is 0.45 nm, whereas the spacing (d_g) on a corrugated gold surface is 0.50 nm.¹⁵ Since the strength of the van der Waals interaction is proportional to the sixth power of the separation

$$\left(\frac{d_b}{d_g}\right)^6 = \left(\frac{4.5}{5}\right)^6 = 0.53 \approx \frac{1}{2} \quad (4)$$

it is expected that the intermolecular potential of dodecane molecules on a gold surface should be about half that of the molecules in bulk. The role of three-body forces is not mentioned here and may also be important.

The model's specular recovery for a molecular coverage of 5% (Figure 5b) shows an asymptotic increase to a value that increases with decreasing temperature, consistent with the equilibrium results (Figure 5a, red trace). An exception is the lowest temperature run, where the molecules become kinetically trapped as soon as they find a single nearest neighbor resulting in a final non-equilibrium specularity. The corrugation potential

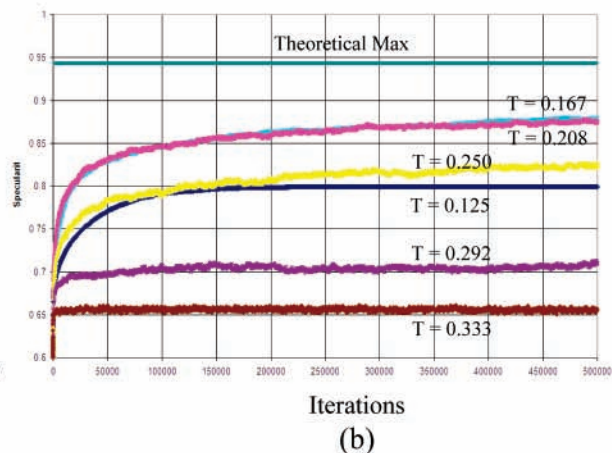


Figure 5. (a) Specularity vs temperature curves generated by the computer model, at specified surface coverages. (b) Specularity vs time (iterations per molecule) curves generated by the computer model for different temperatures. Temperatures are in theoretical units of ϵ/k_B .

is intentionally neglected in the model. Including the corrugation potential would have slowed each simulation by the corresponding Boltzmann factor, greatly encumbering the process. Below, we explain how we are able to extract the corrugation potential by comparing the model to the experimental results. It is also worth noting that the lower temperature recovery curves of Figure 5b show much less thermal fluctuation than those of higher temperature recovery curves.

To determine the value for the corrugation energy of a dodecane molecule on a gold surface, we use the specular recovery versus time curves of the model. The program neglects the corrugation energy when calculating the energy required for a molecule to move from one site to another (which has the effect of simply speeding up the simulated islanding process). The ratio between the experimental recovery rate and that predicted by the model (assuming 10^{-15} s/step) should be the Boltzmann factor (eq 1), where E is the corrugation energy. Hence, we can obtain a rough value for the corrugation energy by comparing the recovery rates for the model and the experimental system.

Using this method, we calculate

$$E_c = 0.3 \pm 0.1 \text{ eV} \quad (5)$$

The fact that the corrugation energy is significantly higher than the intermolecular potential is important. This is consistent with the fact that dodecane molecules pack commensurate on the gold surface at an intermolecular distance that is greater than that in bulk.¹⁵ On the other hand, it is expected that the corrugation energy will be less than the intermolecular potential for molecules that form incommensurate monolayers.

Conclusion

We have used low-energy helium reflectivity to observe island formation and subsequent 2-D sublimation of dodecane molecules on a gold surface at various temperatures and surface

coverages. A Monte Carlo model produced similar results and allowed us to infer the intermolecular potential (0.10 ± 0.03 eV) and corrugation energy (0.3 ± 0.1 eV). This work is helpful in understanding the hierarchy of energies involved in the self-assembly process of organic molecules on metal surfaces, which we found increase in strength for Dodecane on Au(111) accordingly: adsorbate—adsorbate, corrugation of adsorbate on substrate, and adsorbate—substrate.

Acknowledgment. These data were collected in the laboratory of Dr. Giacinto Scoles at Princeton University. Acknowledgment is made to the Donors of the American Chemical Society Petroleum Research Fund for partial support of this research.

References and Notes

- (1) Ulman, A. *An Introduction to Ultrathin Organic Films: From Langmuir-Blodgett to Self-Assembly*; Academic Press, Inc.: San Diego, 1991.
- (2) Ulman, A. *Chem. Rev.* **1996**, *96*, 1533.
- (3) Schreiber, F. *Prog. Surf. Sci.* **2000**, *65*, 151.
- (4) Whitesides, G. M.; Laibinis, P. E. *Langmuir* **1990**, *6*, 87.
- (5) Dubois, L. H.; Nuzzo, R. G. *Annu. Rev. Phys. Chem.* **1992**, *43*, 437.
- (6) Xia, Y. N.; Whitesides, G. M. *Annu. Rev. Mater. Sci.* **1998**, *28*, 153.
- (7) Liu, G. Y.; Xu, S.; Qian, Y. L. *Acc. Chem. Res.* **2000**, *33*, 457.
- (8) Nyffenegger, R. M.; Penner, R. M. *Chem. Rev.* **1997**, *97*, 1195.
- (9) Kramer, S.; Fuierer, R. R.; Gorman, C. B. *Chem. Rev.* **2003**, *103*, 4367.
- (10) Workman, R. K.; Schmidt, A. M.; Manne, S. *Langmuir* **2003**, *19*, 3248.
- (11) Comsa, G.; Poelsma, B. In *Atomic and Molecular Methods*; Scoles, G., Ed.; Oxford University Press: New York, 1992; Vol. 2, Ch. 16.
- (12) Schwartz, P. V.; Schreiber, F.; Eisenberger, P.; Scoles, G. *Surf. Sci.* **1999**, *423*, 208.
- (13) Hemminger, J. et al. *Langmuir* **1987**, *13*, 2318.
- (14) Stranick, S. J.; Kamna, M. M.; Weiss, P. L. *Surf. Sci.* **1995**, *388*, 41.
- (15) Schwartz, P. V.; Lavrich, D. J.; Scoles, G. *Langmuir* **2003**.
- (16) Wetterer, S. M.; Lavrich, D. J.; Cummings, T.; Bernasek, S. L.; Scoles, G. *J. Phys. Chem. B* **1998**, *102*, 92666.